

Synthesis and characterization of a new copper(II) coordination polymer with mixed ligands of tetrabromoterephthalic acid and imidazole

Kodchakorn Samakun¹, Chatphorn Theppitak², Suwadee Jiajaroen², Winya Dungkaew³, Taradon Pirochat⁴, and Kittipong Chainok^{1*}

¹Materials and Textile Technology, Faculty of Science and Technology, Thammasat University, Pathum Thani 12121, Thailand

²Division of Chemistry, Faculty of Science and Technology, Thammasat University, Pathum Thani 12121, Thailand

³Department of Chemistry, Faculty of Science, Mahasarakham University, Mahasarakham 44150, Thailand

⁴Petroleum Authority of Thailand Exploration & Production (PTTEP), Chatuchak, Bangkok 10900, Thailand

*Corresponding author; Email: kc@tu.ac.th

Received 23 September 2019; Revised 22 November 2019; Accepted 2 December 2019
Published online 21 December 2019

Abstract

A new copper(II) coordination polymer containing mixed ligands of tetrabromoterephthalate (Br₄tp) and imidazole (Im), [Cu(Br₄tp)(Im)(H₂O)] (1), was successfully synthesized and characterized by single crystal X-ray diffraction, powder X-ray diffraction, elemental analysis, infrared spectroscopy, and thermogravimetric analysis. The single crystal X-ray diffraction analysis at 100(2) K and 296(2) K revealed that 1 crystallizes in the centrosymmetric monoclinic with space group C2/c, and displays a two-dimensional sheet with a binodal (3,4)-connected net. Compound 1 exhibited thermal stability up to 240 °C.

Keywords: coordination polymer, copper(II), crystal structure, imidazole, mixed ligands, thermal decomposition

1. Introduction

The design and construction of coordination polymers (CPs) by the self-assembly process of metal ions/clusters and polydentate bridging ligands have attracted great attention in the fields of crystal engineering, chemical crystallography and materials chemistry. This is because of their fascinating structural topologies and their potential applications in molecular separation (Duan et al., 2018; Lyu, Zhang, Wang, & Duan, 2018), gas storage (Inukai et al., 2018; Lyu et al., 2018), catalysis (Xue et al., 2018), luminescence (William & Li, 2018; Xue et al., 2018; Li, Yang, Pan, & Liu, 2018), and magnetic (Bai et al., 2018). A key point in the formation and structures of such hybrid organic-inorganic materials is by the judicious choice of building blocks along with tuning synthetic conditions (Faustini, Nicole, Ruiz-Hitzky, & Sanchez, 2018). The variety of coordination geometries accessible to metal ions, diverse structural topologies of CPs have been reported (Zhang et al., 2018). Apart from metal ions, the choice of organic ligands is important in the synthesis of novel CPs and their potential applications (Li et al., 2018). Among various organic ligands, special attention has been paid to the aliphatic and aromatic nitrogen-containing and

oxygen-containing ligands owing to their rich coordination modes upon complexation (Razavi & Morsali, 2019). A combination of chelating nitrogen-donors with carboxylates to promote a specific coordination geometry and assembly motifs of CPs has been attracting increasing interest in recent years. For instance, Dong and co-workers have synthesized a cobalt(II) based porous CP by the combination of a bent imidazole-bridged ligand and benzenedicarboxylic acid under solvothermal conditions (Wang et al., 2015). This porous CP material exhibits a highly active recyclable solid catalyst of various organic substrates. Recently, we have utilized the mixed ligands strategy to synthesize a three-dimensional zinc(II)-barium(II) bimetallic CP and to explore its luminescence properties (Phadungsak et al., 2018; Phadungsak et al., 2019). Moreover, we have found that a one-dimensional copper(II) CP of 4,4'-bipyridine and terephthalate mixed ligands exhibited interesting adsorption-desorption properties (Dungkaew et al., 2019). As a part of our continuous research in exploring novel CPs with the strategy of utilizing the mixed ligands (Chainok et al., 2018). Herein, we report the synthesis, structural characterization, and thermal decomposition of a new copper(II) CP,

[Cu(Br₄tp)(Im)(H₂O)] (**1**), obtained by reacting tetrabromoterephthalic acid (H₂Br₄tp) and imidazole (Im) with copper(II) ion under hydrothermal conditions.

2. Objectives

The main objectives of the present work are as follows: (i) synthesis and structural characterization of novel mixed ligands CPs by using tetrabromodicarboxylate linker and imidazole as ancillary ligand, and (ii) study of its thermal stability.

3. Materials and methods

All chemicals, i.e. Cu(NO₃)₂·3H₂O, tetrabromoterephthalic acid (H₂Br₄tp), and imidazole (Im), were reagent grade and were used without further purification. Powder X-ray diffraction (PXRD) measurements were carried out on a Bruker D8 ADVANCE X-ray powder diffractometer using Cu K α ($\lambda = 1.54178 \text{ \AA}$). The simulated powder patterns were calculated from single crystal X-ray diffraction data and processed by the free Mercury version 3.5.1 program provided by the Cambridge Crystallographic Data Centre (Macrae et al., 2008). FT-IR spectra were recorded on a Perkin-Elmer model Spectrum GX FTIR spectrometer using KBr pellets, in the range of 400-4000 cm⁻¹. Elemental (C, H, N) analysis was determined with a LECO CHNS 932 elemental analyser. Thermogravimetric analyses (TGA) were carried out using a Mettler Toledo TGA/DSC3+ from 30-800 °C with a heating rate of 10 °C/min, under nitrogen atmosphere.

3.1 Preparation of [Cu(Br₄tp)(Im)(H₂O)] (**1**)

A mixture of Cu(NO₃)₂·3H₂O (24 mg, 0.1 mmol), H₂Br₄tp (48 mg, 0.1 mmol), and Im (7 mg, 0.1 mmol) was added to a 15 mL Teflon-lined stainless steel container containing distilled H₂O (5 mL) with vigorous stirring for 30 min. The container was sealed in a stainless-steel autoclave, placed in an oven, and subsequently heated to 120 °C under autogenous pressure for 48 h. The reaction mixture was cooled to room temperature. After filtration,

light blue plate single crystals were obtained in 87% (21 mg) yield based on copper(II) source. Anal. calc. for C₁₁H₆Br₄CuN₂O₅: C, 20.99; H, 0.96; N, 4.45% found: C, 20.75; H, 0.91; N, 4.21%. FT-IR (KBr, ν/cm^{-1} , s for strong, m medium, w weak): 3514w, 3421w, 3149w, 1571s, 1415s, 1324s, 1570s, 1182w, 1069m, 919w.

3.2 X-ray crystallography

A single crystal of **1** with dimensions of 0.30 × 0.22 × 0.18 mm was mounted to the end of a hollow glass fiber. X-ray diffraction data were collected using a Bruker D8 QUEST CMOS PHOTON 200 with graphite monochromated Mo-K α ($\lambda = 0.71073 \text{ \AA}$) radiation at 296(2) K or a Bruker D8 VENTURE CMOS PHOTON 100 with graphite monochromated Cu-K α ($\lambda = 1.54178 \text{ \AA}$) radiation at 100(2) K. Data reduction was performed using SAINT and SADABS scaling algorithm. The software program Bruker, 2016 version (Bruker, APEX3, SADABS and SAINT, 2016. Bruker AXS Inc., Madison, Wisconsin, USA) was used for absorption correction. The structure was solved with the ShelXT structure solution program using combined Patterson and dual-space recycling methods (Sheldrick, 2015a). The structure was refined by least squares using ShelXL (Sheldrick, 2015b). All non-H atoms were refined anisotropically. The H atoms of solvent molecules were positioned geometrically with C–H = 0.93 Å and refined using a riding model (AFIX43 for methyl H atom in ShelXL program) with fixed displacement parameters $U_{\text{iso}}(\text{H}) = 1.5U_{\text{eq}}(\text{C})$. The O–H and N–H hydrogen atoms were located in difference Fourier maps but refined with O–H = 0.84 ± 0.02 Å with $U_{\text{iso}}(\text{H}) = 1.5U_{\text{eq}}(\text{O})$ and N–H = 0.86 ± 0.02 Å with $U_{\text{iso}}(\text{H}) = 1.2U_{\text{eq}}(\text{N})$, respectively. A summary of crystal data and structural refinement parameters for **1** is given in Table 1. Crystallographic data for **1** have been deposited in the Cambridge Crystallographic Data Centre, CCDC numbers 1953713 (100(2) K) and 1953714 (296(2) K).

Table 1 Crystal data and structure refinement for **1** at 100(2) and 296(2) K

Compound	1LT	1RT
CCDC number	1953713	1953714
Empirical formula	C ₁₁ H ₆ Br ₄ CuN ₂ O ₅	C ₁₁ H ₆ Br ₄ CuN ₂ O ₅
Temperature (K)	100(2)	296(2)
Formula weight	629.36	629.36
Crystal size (mm)	0.30 × 0.22 × 0.18	0.30 × 0.22 × 0.18
Crystal System	Monoclinic	Monoclinic
Space Group	C2/c	C2/c
<i>a</i> (Å)	19.1730(12)	19.2151(14)

b (Å)	16.0816(10)	16.1821(11)
c (Å)	9.7483(6)	9.7959(7)
β (°)	91.7780(10)	92.253(3)
V (Å ³)	3004.3(3)	3043.6(4)
Z	8	8
Radiation type	Cu K α ($\lambda = 1.54178$)	Mo K α ($\lambda = 0.71073$)
μ (mm ⁻¹)	14.79	3.63
Diffractometer	BRUKER D8 VENTURE CMOS PHOTON I	BRUKER D8 QUEST CMOS PHOTON II
Absorption correction	multi-scan	multi-scan
θ_{\min} , θ_{\max} (°)	7.176–144.688	6.534–56.912
Index ranges	$-23 \leq h \leq 23$, $-19 \leq k \leq 19$, $-12 \leq l \leq 12$	$-25 \leq h \leq 25$, $-21 \leq k \leq 21$, $-13 \leq l \leq 13$
Reflection collected	21766	47881
Independent Reflections	2962	3814
Reflections [$I > 2\sigma$]	2955	3169
R_{int}	0.0249	0.0602
Data/restraints/parameters	2962/3/221	3814/3/221
R_1 , wR_2	0.0168, 0.0405	0.0284, 0.0570
R_1 , wR_2 (all)	0.0169, 0.0405	0.0408, 0.0609
S	1.23	1.054
$\Delta\rho_{\text{max}}$, $\Delta\rho_{\text{min}}$ (e Å ⁻³)	0.48, -0.43	0.94, -0.86

4. Results and discussion

4.1 Crystal structure

The single crystal X-ray diffraction analysis at 100(2) and 296(2) K revealed that **1** crystallizes in the centrosymmetric triclinic space group $C2/c$. The solid-state structure of **1** is shown in Figure 1. The asymmetric unit contains one copper(II) ion, two half $\text{Br}_4\text{tp}^{2-}$ ligands, one Im ligand, and one coordinated H_2O molecule. The copper(II) center shows a distorted $[\text{CuNO}_4]$ square pyramid coordination geometry which is coordinated by three oxygen atoms from different $\text{Br}_4\text{tp}^{2-}$ ligands, one nitrogen

atom from Im ligand, and one oxygen atom from coordinated water molecule. The bond angles around the $[\text{CuNO}_4]$ square pyramidal geometry range from $86.30(7)$ – $175.13(8)^\circ$ and $85.72(11)$ – $175.64(11)^\circ$ at 100(2) and 296(2) K, respectively, Table 2. The Cu–N and Cu–O bond lengths at both temperatures are not significantly different *viz.* $1.946(2)$ – $2.276(2)$ Å at 100(2) K and $1.945(3)$ – $2.299(2)$ Å at 296(2) K (Table 2), and are in the range of the typical Cu–N and Cu–O bond lengths previously reported (Cati & Stoeckli-Evans, 2014).

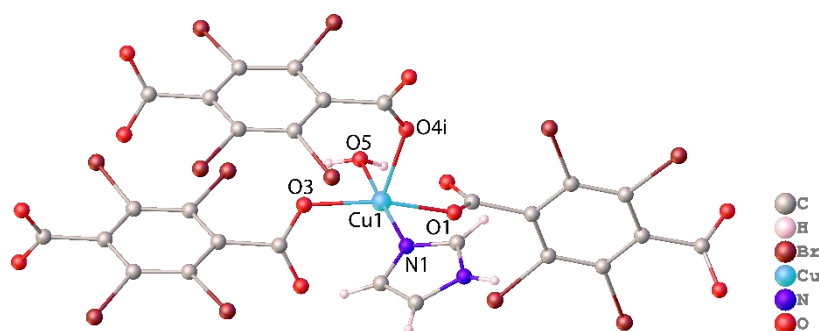


Figure 1 Coordination environment of copper(II) ion in **1**. Symmetry code: (i) $x, 1 - y, -0.5 + z$

Table 2 Bond lengths and bond angles (Å, °) for **1** at 100(2) and 296(2) K

Bond lengths (Å)	100(2) K	296(2) K
Cu1–O1	2.006(2)	2.003(2)
Cu1–O3	1.972(2)	1.968(2)
Cu1–O4 ⁱ	2.276(2)	2.299(2)
Cu1–O5	1.982(2)	1.978(3)
Cu1–N1	1.946(2)	1.945(3)
Bond angles (°)		
O1–Cu1–O4 ⁱ	95.38(6)	96.36(10)
O3–Cu1–O1	164.42(7)	164.03(10)
O3–Cu1–O4 ⁱ	99.96(6)	99.36(9)
O3–Cu1–O5	87.05(7)	87.18(10)
O5–Cu1–O1	88.58(7)	88.43(10)
O5–Cu1–O4 ⁱ	96.19(7)	95.94(11)
N1–Cu1–O1	87.02(8)	87.38(11)
N1–Cu1–O3	96.66(8)	96.53(11)
N1–Cu1–O4 ⁱ	86.30(7)	85.72(11)
N1–Cu1–O5	175.13(8)	175.64(11)
Symmetry code: (i) $x, -y + 1, z - 0.5$		

The Br₄tp²⁻ ligands are fully deprotonated with respect to the carboxylic acid groups under hydrothermal conditions and display a bidentate μ_2 - η^1 : η^1 -bridging mode and a tetradentate μ_4 - η^1 : η^1 : η^1 : η^1 -bridging mode. As can be seen in Figure 2, the copper(II) ions are bridged by Br₄tp²⁻ ligands to afford a two-dimensional sheet in the *ac* plane. While, the Im ligand binds to copper(II) ion in a monodentate fashion. The Cu...Cu separation

within the sheets is in the range from 4.9376(3) to 10.9314(7) Å. It should be noted that the intramolecular O–H...Br and O–H...O hydrogen bonds are observed within the sheets, Table 3. From the topological view, the Br₄tp²⁻ ligands can be regarded as 2- and 4-connected nodes. Cu1 ion is attached to three Br₄tp²⁻ ligands and can be considered as a 3-connected node. Thus, **1** possesses a binodal (3,4)-connected net as shown in Figure 3.

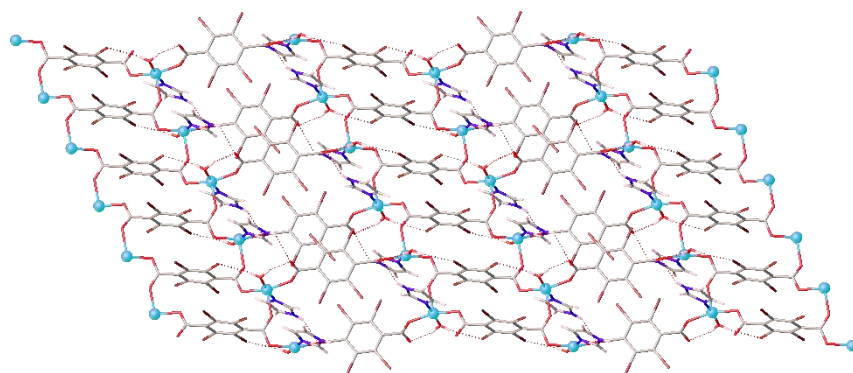


Figure 2 A view of the two-dimensional sheet of **1** in the *ac* plane

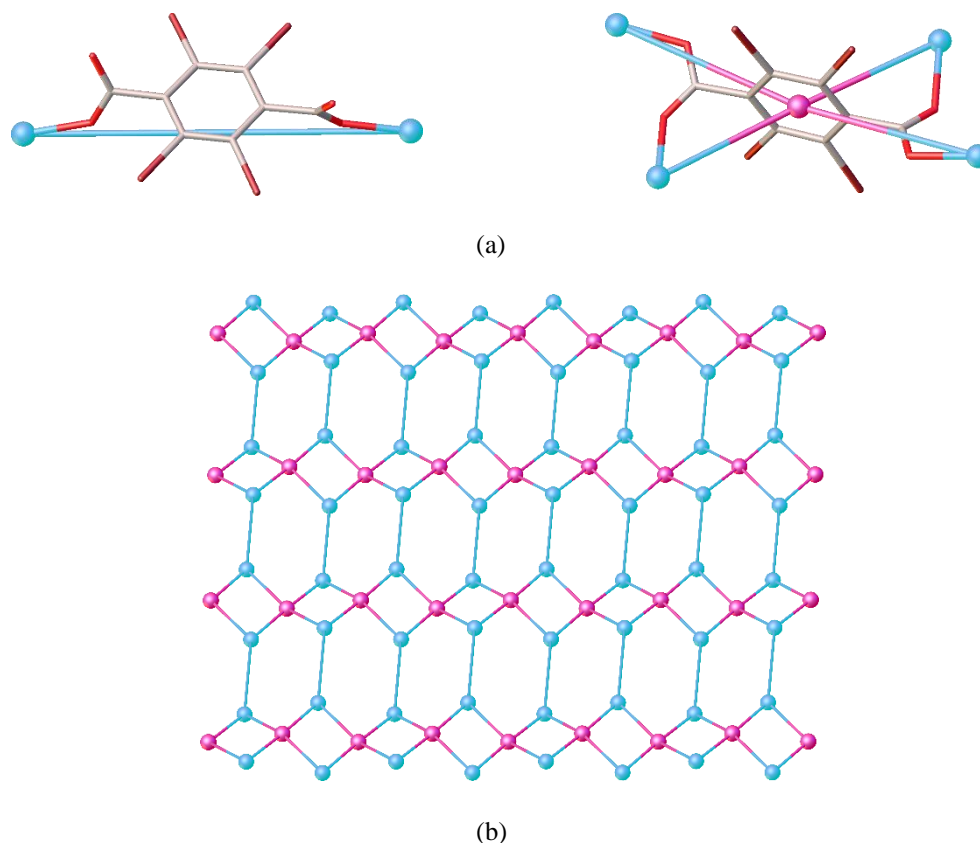


Figure 3 (a) The simplification of $\text{Br}_4\text{tp}^{2-}$ ligands and (b) schematic representation of (3,4)-connected net along the ac plane for **1**

The two-dimensional sheets are packed in an offset fashion. There are strong bifurcated $\text{N-H}\cdots\text{O}$ hydrogen bonds involving the Im ligands and the coordinated water molecules and the carboxyl groups from $\text{Br}_4\text{tp}^{2-}$ ligands (Table 3). It should be noted that stronger intermolecular interactions are known to be less affected by temperature (Chongboriboon et al., 2020). In this study, lowering the temperatures from 296(2) K to 100(2) K does not lead to any significant differences in the interactions. Moreover, $\text{Br}\cdots\text{O}$ ($\text{Br}\cdots\text{O} =$

3.138(2) at 100(2) K and 3.140(5) at 296(2) K) and $\text{Br}\cdots\text{Br}$ ($\text{Br}\cdots\text{Br} = 3.595(2)$ at 100(2) K and 3.601(5) at 296(2) K) halogen bonding interactions are also observed along with the additional $\text{Br}\cdots\pi$ interaction involving the bromine atom and the centroid (Cg) of Im molecule ($\text{Br}\cdots\text{Cg} = 3.279(2)$ and 3.288(4) Å at 100(2) and 296(2) K, respectively). A combination of these intermolecular interactions linked the two-dimensional sheets into the three-dimensional supramolecular structure and these interactions help stabilize the framework.

Table 4 Hydrogen-bond geometry (Å, °) for **1** at 100(2) and 296(2) K

$D-H\cdots A$	$D-H$		$H\cdots A$		$D\cdots A$		$D-H\cdots A$	
	100(2) K	296(2) K	100(2) K	296(2) K	100(2) K	296(2) K	100(2) K	296(2) K
$\text{O5-H5A}\cdots\text{Br3}$	0.83(2)	0.82(2)	2.54(2)	2.55(2)	3.353(2)	3.362(3)	170(4)	171(5)
$\text{O5-H5B}\cdots\text{O2}$	0.83(2)	0.83(2)	1.80(2)	1.81(3)	2.605(2)	2.607(3)	163(4)	161(5)
$\text{N2-H2}\cdots\text{O2}^i$	0.87(2)	0.85(2)	2.40(3)	2.43(4)	3.002(3)	3.033(4)	126(3)	128(4)
$\text{N2-H2}\cdots\text{O5}^{ii}$	0.87(2)	0.85(2)	2.51(3)	2.55(4)	3.012(3)	3.073(4)	118(3)	121(4)

Symmetry code: (i) $x, -y + 1, z - 1/2$, (ii) $1.5 - x, -1/2 + y, 1/2 - z$

4.2 PXRD, IR, and TG analysis

The phase purity of **1** was confirmed by powder X-ray diffraction at room temperature. As shown in Figure 4, the peak positions of the experimental and simulated patterns are in agreement with each other, confirming the good phase purity of **1**. It can be noted that due to the variation in preferred orientation of the crystalline samples during the PXRD data collection, the reflection intensities of the simulated pattern were different from that of the experimental pattern.

The FT-IR spectrum of **1** is shown in Figure 5. The characteristic bands of the deprotonated carboxylate groups of $\text{Br}_4\text{tp}^{2-}$ ligand are shown in the range $1526\text{--}1562\text{ cm}^{-1}$ for asymmetric stretching and $1317\text{--}1408\text{ cm}^{-1}$ for symmetric stretching (Li et al., 2012). The vibration bands in the region of $\sim 3153\text{--}3510\text{ cm}^{-1}$ correspond to the N–H stretching of the Im ligands and the O–H stretching of coordinated H_2O molecules. The characteristic bands of the aromatic C=C and the C–H vibration are also observed around $1400\text{--}1570$ and $920\text{--}1000\text{ cm}^{-1}$, respectively. The FT-IR spectrum was

consistent with their structural characteristics as determined by single crystal X-ray diffraction analysis.

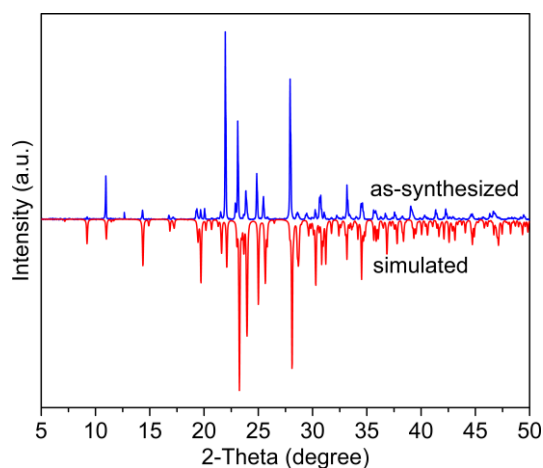


Figure 4 Comparison of the as-synthesized PXRD pattern of **1** at room temperature with the simulated diffraction pattern from the single crystal X-ray structure determination

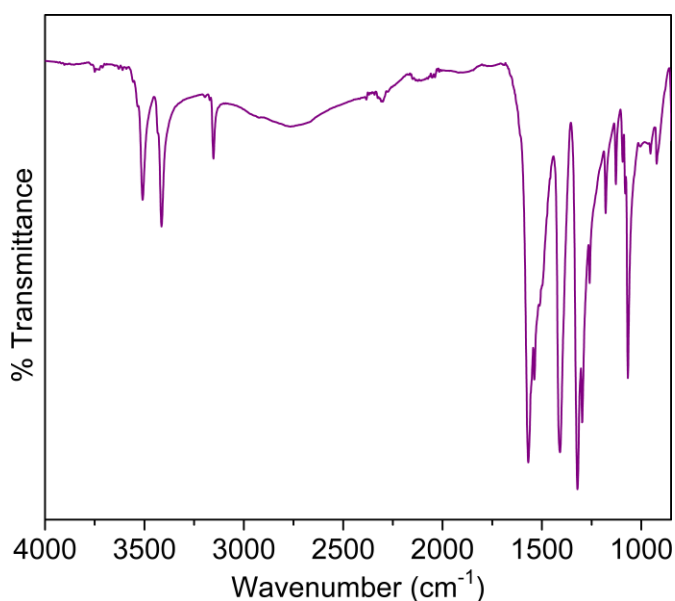


Figure 5 FT-IR spectrum for **1** in the solid-state at room temperature

The thermal behavior of **1** was investigated under a N_2 atmosphere from $30\text{--}800\text{ }^\circ\text{C}$ and the result is shown in Figure 6. There is no weight loss from 30 to $240\text{ }^\circ\text{C}$, possibly due to the strong hydrogen

bonding and halogen bonding interactions between the two-dimensional sheets as discussed above. The second weight loss above $240\text{ }^\circ\text{C}$ corresponds to the decomposition of coordination network of **1**.

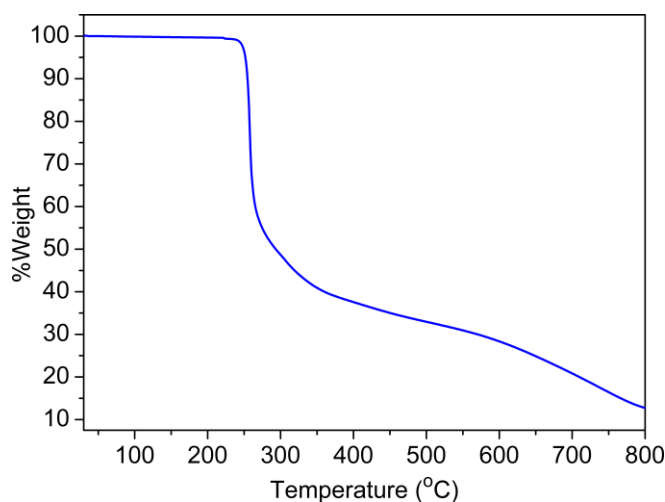


Figure 6 TG curve of **1**

5. Conclusion

In summary, a new copper(II) CP, [Cu(Br₄tp)(Im)(H₂O)] (**1**) was successfully synthesized from mixed organic ligands of tetrabromoterephthalic acid and imidazole under hydrothermal conditions. The network structure of **1** is directed by the coordination modes of Br₄tp²⁻ ligands, resulting in a two-dimensional (3,4)-connected sheets. Through a combination of hydrogen bonding and halogen bonding interactions, the sheets are held together into the three-dimensional supramolecular structure. The framework of **1** is thermally stable up to 240 °C. The results in the present study indicate that the mixed-ligand strategy may be an efficient approach to constructing multidimensional CPs with interesting properties for many potential applications. Efforts along this line are underway in our laboratory.

6. Acknowledgements

The authors thank the Faculty of Science and Technology, Thammasat University, for funds to purchase the X-ray diffractometer. K.S. acknowledges the NSTDA STEM Workforce (SCA-CO-2560-5118-TH) and the National Research Council of Thailand (contact No. 03/2562) for financial support.

7. References

- Bai, N., Gao, R., Wang, H., Wu, Y., Hou L., & Wang, Y.-Y. (2018). Five transition metal

coordination polymers driven by a semirigid trifunctional nicotinic acid ligand: selective adsorption and magnetic properties. *CrystEngComm*, 20, 5726-5734. DOI: 10.1039/C8CE01003J

Cati, D. S., & Stoeckli-Evans, H. (2014). Crystal structure of poly[[acetato-κO]{μ₃-N-[(pyridin-4-yl)methyl]pyrazine-2-carboxamidato-κ⁴N¹,N²:N⁴}copper(II)] dihydrate]: a metal-organic framework (MOF). *Acta Crystallographica Section C*, E70, 23-26. DOI: 10.1107/S1600536814011520

Chainok, K., Ponjan, N., Theppitak, C., Khemthong, P., Kielar, F., Dungkeaw, W., . . . Batten, S. (2018). Temperature-dependent 3D structures of lanthanide coordination polymers based on dicarboxylate mixed ligands. *CrystEngComm*, 20, 7446-7457. DOI: 10.1039/C8CE01430B

Chongboriboon, N., Samakun, K., Inprasit, T., Dungkeaw, W., Kielar, F., Wong, L. H.-Y., . . . Chainok, K. (2020). Two-dimensional halogen-bonded organic frameworks based on the tetrabromobenzene-1,4-dicarboxylic acid building molecule. *CrystEngComm*, 22, 24-34. DOI: 10.1039/C9CE01140D

Duan, J., Zhang, Q., Wang, S., Zhou, B., Sun, J., & Jin, W. (2018). Controlled flexibility of porous coordination polymers by shifting

- the position of the $-\text{CH}_3$ group around coordination sites and their highly efficient gas separation. *Inorganic Chemistry Frontiers*, 5, 1780-1786. DOI: 10.1039/C8QI00240A
- Dungkaew, W., Jiajaroen, S., Theppitak, C., Sertphon, D., & Chainok, K. (2018). Copper (II) adsorption property of 1D coordination polymer $[\text{Cu}_2(\text{H}_2\text{O})(\text{bipy})_2(\text{tp})_2]$ (bipy = 2,2'-bipyridine, tp = terephthalate) after acid treatment. *Journal of Current Science and Technology*, 9(1), 29-39.
- Faustini, M., Nicole L., Ruiz-Hitzky, E., & Sanchez, C. (2018). History of organic-inorganic hybrid materials: prehistory, art, science, and advanced applications. *Advanced Functional Materials*, 28(27), 1704158-1704188. DOI: 10.1002/adfm.201704158
- Inukai, M., Tamura, M., Horike, S., Higuchi, M., Kitagawa, S., & Nakamura, K. (2018). Storage of CO_2 into porous coordination polymer controlled by molecular rotor dynamics. *Angewandte Chemie, International Edition*, 57(28), 8687-8690. DOI: 10.1002/anie.201805111
- Li, G., Yang, Q., Pan, R., & Liu, S. (2018). Diverse cobalt (II) coordination polymers for water/ethanol separation and luminescence water sensing applications. *CrystEngComm*, 20, 3891-3897. DOI: 10.1039/C8CE00709H
- Li, L., Wang, S., Chen, T., Sun, Z., Luo, J., & Hong, M. (2012). Solvent-dependent formation of Cd(II) coordination polymers based on a C_2 -symmetric tricarboxylate linker. *Crystal Growth & Design*, 12(8), 4109-4115. DOI: 10.1021/cg300617h
- Li, N., Feng, R., Zhu, J., Chang, Z., & Bu, X.-H. (2018). Conformation versatility of ligands in coordination polymers: From structural diversity to properties and applications. *Coordination Chemistry Reviews*, 375, 558-586. DOI: doi.org/10.1016/j.ccr.2018.05.016
- Lyu, H., Zhang, Q., Wang, Y., & Duan, J. (2018). Unified meso-pores and dense Cu^{2+} sites in porous coordination polymers for highly efficient gas storage and separation. *Dalton Transactions*, 47, 4424-4427. DOI: 10.1039/C8DT00512E
- Macrae, C. F., Bruno, I. J., Chisholm, J. A., Edgington, P. R., McCabe, P., Pidcock, E., . . . Wood, P. A. (2008). Mercury CSD 2.0 - new features for the visualization and investigation of crystal structures. *Journal of Applied Crystallography*, 41(Pt 2), 466-470. DOI: 10.1107/S0021889807067908
- Phadungsak, N., Boonyuen, S., Sertphon, D., Dungkaew, W., Kielar, F., & Chainok, K. (2018). A new three-dimensional zinc(II)-barium(II) coordination polymer based on trimesic acid and imidazole ligands: synthesis, structure and properties. *Journal of Current Science and Technology*, 8(1), 1-9. DOI: 10.14456/jcst.2018.1
- Phadungsak, N., Kielar, F., Dungkaew, W., Sukwattanasinitt, M., Zhou, Y., & Chainok, K. (2019). A new luminescent anionic metal-organic framework based on heterometallic zinc(II)-barium(II) for selective detection of Fe^{3+} and Cu^{2+} ions in aqueous solution. *Acta Crystallographica Section C*, 75(Pt 10), 1372-1380. DOI: 10.1107/S2053229619011987
- Razavi, S. A. A., & Morsali, A. (2019). Linker functionalized metal-organic frameworks. *Coordination Chemistry Reviews*, 399, 213023-213057. DOI: 10.1016/j.ccr.2019.213023
- Sheldrick, G. M. (2015a). SHELXT - Integrated space-group and crystal-structure determination. *Acta Crystallographica Section A: Foundations and Advances*, 71(Pt 1), 3-8. DOI: 10.1107/S2053273314026370
- Sheldrick, G. M. (2015b). Crystal structure refinement with SHELXL. *Acta Crystallographica*, C71, 3-8. DOI: 10.1107/S2053229614024218
- Wang, J.-C., Ding, F.-W., Ma, J.-P., Liu, Q.-K., Cheng, J.-Y., & Dong, Y.-B. (2015). Co(II)-MOF: A highly efficient organic oxidation catalyst with open metal sites. *Inorganic Chemistry*, 54(22), 10865-10872. DOI: 10.1021/acs.inorgchem.5b01938

- William, P. L., & Li, J. (2018). Luminescent metal–organic frameworks and coordination polymers as alternative phosphors for energy efficient lighting devices. *Coordination Chemistry Reviews*, 373, 116-147. DOI: 10.1016/j.ccr.2017.09.017
- Xue, L.-P., Li, Z.-H., Zhang, T., Cui, J.-J., Gao, Y., & Yao, J.-X. (2018). Construction of two Zn(II)/Cd(II) multifunctional coordination polymers with mixed ligands for catalytic and sensing properties. *New Journal of Chemistry*, 42, 14203-14209. DOI: 10.1039/C8NJ02055H
- Zhang, Q.-L., Yu, Q., Xie, H.-F., Tu, B., Xu, H., Huang, Y.-L., & Yang, X.-S. (2018). Structural diversity of six coordination polymers based on the designed X-shaped ligand 1,1,1,1-tetrakis[(3-pyridiniourea)methyl]methane. *Molecules*, 23(9), 2292-2305. DOI: 10.3390/molecules23092292